A discrete wave number transform approach for predicting pressure levels due to a line source radiating over two dimensional multi-layered materials

Stéphane Rigobert, Franck Sgard, Claude Boutin

A discrete wave number transform approach for predicting pressure levels due to a line source radiating over two dimensional multi-layered materials

S. Rigobert [a,*], F. Sgard [a], C. Boutin [b]

[a] *Laboratoire des Sciences de l'Habitat, Department of civil Engineering and Buildings, URA CNRS 1652 Ecole nationale des Travaux publics de l'Etat, 2 rue Maurice Audin, 69518 Vaulx en Velin, France*
[b] *Laboratoire Geomatériaux, DGCB, URA CNRS 1652, Ecole nationale des Travaux publics de l'Etat, 2 rue Maurice Audin, 69518 Vaulx en Velin, France*

Abstract

The problem of an acoustical line source radiating over a planar multi layered material infinite in two of its dimensions, made up of acoustic, elastic and porous media is investigated. The fields in the different media are expanded into a superposition of plane waves using a one dimensional spatial Fourier transform along the material's interface. The problem amounts to solving for the reflection and transmission coefficients of the plane waves at each interface. The contributions of each wave are then recombined using the discrete wave number method, referred to as Bouchon's method, to get the fields in the media. The results given by the developed algorithm are successfully compared to an analytical solution considered for pro pagation above a locally reacting plane.

Keywords: Porous media; Multi layered materials; Line sources; Wave number decomposition.

1. Introduction

In building acoustics, multi-layered materials involving porous media allow for the satisfaction of new standards and an answer to the growing concern about inner acoustical comfort, thanks to their damping properties. In environmental acoustics, porous materials are commonly used on noise barriers or in external protections of

* Corresponding author. Tel.: 00 33 4 72 94 70 66; fax: 00 33 4 72 04 71 56; e mail: secretariat.lash @entpe.fr

buildings against outdoor noise. This trend of a widespread use of porous materials highlights the need of tools allowing for the prediction of their response to several kinds of excitations. From a scientific point of view, a better understanding of the vibro-acoustic behavior of these materials is of great interest. Practically, industrials and design departments use porous media in multi-layered materials in their wish to develop high acoustical performance products. Therefore, there is a need for evaluating their efficiency.

Different models have been proposed to depict a porous material, considering the fluid phase displacement. If the solid phase of a porous medium is assumed motionless, the wave propagates only through the fluid phase. This approach is valid for an acoustical excitation above a decoupling frequency [1] beyond which the two phases of a porous material are then considered to be uncoupled. The assumption of a motionless frame has allowed quite accurate descriptions of the response of porous materials such as soils. Sabatier et al. [2] found that semi-infinite sandy soils excited by a plane wave could be correctly modeled using an equivalent fluid model. In that particular case, frame motion appeared to have no influence on the computed surface impedance. On the other hand, this hypothesis is not valid anymore when considering some hard backed finite foams for example. Some results by Allard [3] for a plane wave excitation show that an equivalent fluid model is unable to depict phenomena such as quarter-wave resonance. Tooms [4] also showed the greater accuracy of elastic-porous models for the prediction of response of low-density foams to a point source excitation. Hence, it seems that even for the case of acoustic excitations, taking into account the elastic frame motion is necessary. Besides, equivalent fluid models are obviously inappropriate in the case a mechanical force excitation, since the solid phase is directly stimulated.

Problems involving plane wave excitations are easier to solve than those considering a volume source or a mechanical excitation for example. In that way, this kind of excitation has been mainly considered. Studies on two-dimensional configurations have been made in the case of impinging plane-waves using a complete description of porous media. Sabatier et al. [2] proposed a description of a porous material based on a modified form of the Biot–Stoll [5] equations. Considering a finite thickness porous material backed by a rigid wall, they applied the boundary conditions between the air and the porous medium in order to get the amplitude coefficients of the propagating waves in the porous medium. Allard [3] used a formalism allowing replacement of a material layer by a *transfer matrix* linking the stresses and velocities at each side of the given layer, so that a surface impedance could be computed. The utility of this latter method lies in the characterization of a porous layer by one matrix. Hence, velocities and stresses can be linked at each side of a multi-layered material by merging layer matrices into a global matrix. Other works based on a finite element model have been achieved for multi-layers of finite lateral size. Bolton and Kang [6] were interested in solving the coupled elasto-poro-acoustic two-dimensional problem of a porous material excited by an impinging plane wave under normal incidence. Also, Panneton and Atalla [7] used a formulation involving the solid and fluid phase displacement (known as the $\{u,U\}$ formulation) to describe the porous material in the case of a coupled elasto-poro-acoustic

three dimensional problem. They applied their theory to the study of the transmission loss of a double plate with a porous material in between. Recently, these authors [8] have developed a $\{u,P\}$ formulation for the porous material using the solid phase displacement and the air pressure in the pores.

Apart from the plane wave excitation, the acoustic field due to a point source over an impedance plane has been investigated. In the case of a locally reacting material [9,10] or an equivalent fluid [11], analytical solutions or approximations by series or integrals have been obtained for three dimensional cases. The problem induced by a volume source radiating over a porous layer has also been solved when considering the elasticity of the frame in the porous medium [12,13]. The axisymmetric displacement potentials are expressed as inverse Hankel transforms. Each of these Hankel transforms stand for plane-wave displacement potentials in the porous medium and are determined by boundary conditions at the interface. Attenborough [12] proposed a heuristic approach to compute the solution expressed in an integral form. This approach gives reasonable accuracy though not completely rigorous. Fast Fourier techniques have also been developed to compute these axisymmetric displacement potentials. These methods, known as Fast Fourier Program methods (FFP programs) initially introduced by DiNapoli and Davenport [14], have been successfully applied to problems of sound propagation in a system composed of a horizontally stratified fluid overlying a horizontally stratified elastic and porous solid [13].

Two dimensional models have also been developed for line source excitations. For the propagation above a flat interface, analytic solutions can be found by considering a porous material depicted as locally reacting [15]. This kind of problem has also been studied for geophysical applications in water saturated stratified soils [16] using a $\{u,P\}$ formulation for the description of the porous material.

In this paper, the two dimensional problem of an acoustical line source radiating over a planar multi-layers infinite in two of its dimensions will be investigated. The line source above a flat interface model is often relevant in building acoustics (e.g., fluid conveying ducts radiating noise near a multi-layered wall) and environmental acoustics (traffic noise in presence of a ground). The method used is the discrete wave number method, referred as Bouchon's method. Initially, this method has been designed in seismic sciences for the computing of the response of an horizontal set of layers to seismic excitations in the case of complicated shaped grounds [17]. In the present work, the method is adapted to an acoustic problem in the case of a planar interface. This approach looks like FFP in its formulation, but is rather different in its physical content. Moreover, a Fourier transform is used instead of a Hankel transform. Finally, Bouchon's method can be extended to more complicated profile for the interface between air and the poroelastic material.

2. Theory

The cases studied in this paper consider an infinitely extended planar multi-layered material made up of acoustic, elastic, and poroelastic media. The equations governing

the wave propagation in the media involved are presented in the following, assuming an $\exp(j\cdot\omega\cdot t)$ time dependence. These equations, valid for a general three dimensional case, are used in the next section for a two-dimensional configuration.

2.1. The propagation equations

2.1.1. In the fluid

The propagation of a wave in a fluid is governed by Helmholtz equation

$$\nabla^2 p(M) + k_f^2 \cdot p(M) = s(M - M_0), \tag{1}$$

where $p(M)$ denotes the pressure at point $M(x,z)$, $k_f = \omega/C_f$ is the wave number in the fluid, C_f the sound speed in the fluid, $s(M-M_0)$ a line source located in $M_0(x_0,z_0)$.

2.1.2. In the porous material

Porous materials are described by Biot–Allard equations [3], and are rewritten here using the frame displacement $\vec{U}_s$ and pressure p inside the pores as variables. When there is no source in the porous material, the equations are as follows:

For the solid phase

$$\begin{aligned} &-\omega^2 \cdot \left[\left(\tilde{\rho}_{11} - \frac{\tilde{\rho}_{12}^2}{\tilde{\rho}_{22}} \right) \cdot \vec{U}_S + \frac{\Phi \cdot \tilde{\rho}_{12}}{\tilde{\rho}_{22} \cdot \omega^2} \cdot \nabla p \right] = (P + Q - N) \nabla\nabla \cdot \vec{U}_S \\ &+ N \nabla^2 \vec{U}_S + Q \cdot \frac{\Phi}{\tilde{\rho}_{22} \cdot \omega^2} \nabla\nabla \cdot \nabla p, \end{aligned} \tag{2}$$

For the fluid phase

$$-\Phi \cdot \nabla p = \frac{R \cdot \Phi}{\tilde{\rho}_{12} \cdot \omega^2} \nabla\nabla \cdot \nabla p + \left(Q - \frac{R \cdot \tilde{\rho}_{12}}{\tilde{\rho}_{22}} \right) \nabla\nabla \cdot \vec{U}_S, \tag{3}$$

where N, P, Q, R denote Biot coefficients which are characteristics of the porous material. These coefficients depend on the bulk modulus of the fluid K_f, the bulk modulus of the elastic solid K_s, the bulk modulus of the frame K_b, and shear modulus μ (Lamé coefficient). Thermal dissipative effects are taken into account through a correcting function $G(B^2\omega)$ introduced in K_b, where B^2 is the Prandtl number.

$\tilde{\rho}_{11}$ and $\tilde{\rho}_{22}$ are the effective densities representing the densities of each phase modified so as to take into account dissipative viscous and inertial effects. $\tilde{\rho}_{12}$ is an effective density accounting for the coupling between both phases. The correcting factor $G(\omega)$ is introduced to include the viscous effects, G being the same function as previously.

The expressions of the effective densities are:

$$\tilde{\rho}_{11} = (1 - \Phi)\rho_S + \rho_a - j\cdot\sigma\cdot\Phi^2\cdot\frac{G(\omega)}{\omega}, \tag{4}$$

$$\tilde{\rho}_{22} = \Phi\cdot\rho_f + \rho_a - j\cdot\sigma\cdot\Phi^2\cdot\frac{G(\omega)}{\omega}, \tag{5}$$

$$\tilde{\rho}_{12} = -\rho_a + j\cdot\sigma\cdot\Phi^2\cdot\frac{G(\omega)}{\omega}, \tag{6}$$

with

$$\rho_a = -\Phi\cdot\rho_f\cdot(\alpha_\infty - 1) \tag{7}$$

representing the inertial coupled effects. ρ_f and ρ_S are the fluid and in the above equations, the solid density, σ is the flow resistivity Φ is the porosity, $_\infty$ is the tortuosity of the porous material.

The system formed by Eqs. (2) and (3) is solved by expressing the displacement fields as a sum of a compressional and a rotational wave. Using this expansion, two kinds of compressional waves (P_1, P_2) and one kind of shear wave are shown to propagate simultaneously in the porous material. For the restricting case of a motionless frame, the porous material is reduced to its fluid phase and is then governed by an Helmholtz-like equation obtained from Eq. (3). In that case, only one compressional wave P_2 can propagate.

2.1.3. In the elastic material

Using $\vec{U}$ as the displacement field of the elastic material, the displacement equation of motion is given by

$$(\lambda + \mu)\nabla\nabla\cdot\vec{U} + \mu\cdot\nabla^2\vec{U} + \rho\cdot\omega^2\cdot\vec{U} = 0, \tag{8}$$

where λ and μ are the Lame coefficients, ρ is the density of the material.

In this case, the expansion in terms of propagation modes highlight the possibility for one kind of compressional wave and one kind of shear wave to propagate.

2.2. General response at a receiver

In the following, the two dimensional problem of a multi-layered material excited by a harmonic line source located in the air is considered. As stated in the introduction, the approach is based on a one-dimensional spatial Fourier transform. The response $\vec{\Re}^i_\omega(M, M_0)$ in medium i at receiver M due to an harmonic acoustical line source located in M_0 and its one-dimensional Fourier transform $\hat{\vec{\Re}}^i(k_x, z)$ are linked by the following equation:

$$\hat{\vec{\Re}}^{i}_{\omega}(M, M_0) = \int_{\infty}^{+\infty} \exp\left(-\mathrm{i}\cdot k_x\cdot\left(x^M - x^{M_0}\right)\right)\cdot \hat{\vec{\Re}}^{i}\left(k_x, z^M - z^{M_0}\right)\cdot \mathrm{d}k_x. \tag{9}$$

In the following, $\left(\hat{f}\right)$ denotes the Fourier transform of f along x. For a porous medium $\hat{\vec{\Re}}(k_x, z^M)\begin{Bmatrix} \vec{U}_s \\ \hat{P} \end{Bmatrix}$, for an elastic medium $\hat{\vec{\Re}}(k_x, z^M) = \begin{Bmatrix} \hat{\vec{U}}_s \end{Bmatrix}$ and for a fluid $\hat{\vec{\Re}}(k_x, z^M) = \hat{P}$.

The quantity $\exp(-i\cdot k_x\cdot(x^M - x^{M_0}))\cdot\hat{\vec{\Re}}(k_x, z^M - z^{M_0})$ in Eq. (9) can be seen as the superposition of all plane wave components with wave-number $\delta = \omega/C_i$ (C_i velocity of the considered kind of wave in the medium) and horizontal wave number k_x.

One needs now to evaluate $\hat{\vec{\Re}}(k_x, z^M - z^{M_0})$ in each medium i.

2.2.1. Response in air for an acoustical line source excitation

In free field conditions the Green's function for the pressure due to a line source in air associated with Helmholtz equation is [17]

$$\frac{H_0^2(\delta_f\cdot -M_0|)}{4\cdot\mathrm{i}} = \int_{\infty}^{+\infty} \frac{1}{4\cdot\mathrm{i}\cdot\pi\cdot k_z}\exp\left(-\mathrm{i}\cdot k_x\cdot\left(x^M - x^{M_0}\right)\right)\cdot\exp\left(-\mathrm{i}\cdot k_z\cdot^M - z^{M_0}|\right)\cdot \mathrm{d}k_x, \tag{10}$$

where H_0^2 is the zero order Hankel's function of the second kind, k_z denotes the vertical wave number in air with $k_z^2 = (\delta_f)^2 - k_x^2$.

Both propagating ($k_x < \omega/C_f$) and evanescent waves ($k_x > \omega/C_f$) are considered.

In presence of a material, the incident plane wave contribution is reflected and refracted. The response in air can be deduced from Eqs. (9) and (10) and written as follows.

$$\hat{\Re}^a(k_1, M) = \frac{1}{4\cdot\mathrm{i}\cdot\pi\cdot k_z}\cdot\left[\exp\left(-\mathrm{i}\cdot k_z\cdot^M - z^{M_0}|\right) + R(k_x)\cdot\exp\left(-\mathrm{i}\cdot k_z\cdot^M + z^{M_0}|\right)\right], \tag{11}$$

where $R(k_x)$ is the plane wave reflection coefficient on the air-multilayered material interface which only depends of the horizontal wave number k_x. $R(k_x)$ has the usual sense for propagating waves, and this notion is extended to evanescent waves [18].

2.2.2. Response in a multi-layered material for a line source

To simplify, the case of a single material of thickness h and backed by a rigid wall is considered (Fig. 1). The principle of the method presented in this section can be extended to a large number of materials. The calculation will be detailed for the case

of one porous material. The main aspects of the method can be reused for an elastic material or a fluid.

In a porous material, the fields can be expanded in propagation modes (compressional and shear waves), to give

$$\hat{\vec{\Re}}_{\omega}^{\text{porous}}(k_x, z^M) = \left\{ \begin{array}{l} \hat{\vec{U}}_{\text{S}} = \nabla\hat{\phi}_1^{\uparrow} + \nabla\hat{\phi}_1^{\downarrow} + \nabla\hat{\phi}_2^{\uparrow} + \nabla\hat{\phi}_2^{\downarrow} + \nabla \wedge \left(\hat{\vec{\psi}}^{\uparrow} + \hat{\vec{\psi}}^{\downarrow}\right) \\ \hat{P} = \frac{1}{\beta}\left((\alpha - \Phi)\nabla\hat{\vec{U}}_{\text{S}} + \Phi\nabla\hat{\vec{U}}_{\text{f}}\right) \end{array} \right\} \tag{12}$$

with $\alpha = 1 - \tilde{K}_{\text{b}}/K_{\text{S}}$ and $\beta = (\alpha - \Phi)/K_{\text{S}} + \Phi/\tilde{K}_{\text{b}}$.

One shall note that the fluid phase displacement $\vec{U}_{\text{f}}$ can be expressed as $\hat{\vec{U}}_{\text{f}} = \mu_1 \cdot \nabla\hat{\phi}_1 + \mu_2 \cdot \nabla\hat{\phi}_2 + \mu_3 \cdot \nabla\hat{\vec{\psi}}$, where μ_i ($i = 1,3$) denote complex amplitude ratio of the fluid displacement over the solid displacement associated with each kind of wave. Expressions for μ_i are given in Ref. [17]. Each scalar potential ($\hat{\phi}_i^{\uparrow}$ for ascending wave and $\hat{\phi}_i^{\downarrow}$ for descending waves) or vectorial potential ($\hat{\vec{\psi}}^{\uparrow}$ for ascending waves and $\hat{\vec{\psi}}^{\downarrow}$ for descending waves) involved in the solid displacement expression may be expressed using the transmission coefficients in the porous medium.

For P *waves*

$$(i = 1, 2) : \phi_{\text{i}} = \frac{A_i(k_x)}{4\text{i}\pi k_z^{\text{P}_{\text{i}}}} \exp\left(-\text{i}k_z^{\text{P}_{\text{i}}} M - \epsilon \cdot z^{M_0}|\right). \tag{13}$$

For an S *wave*

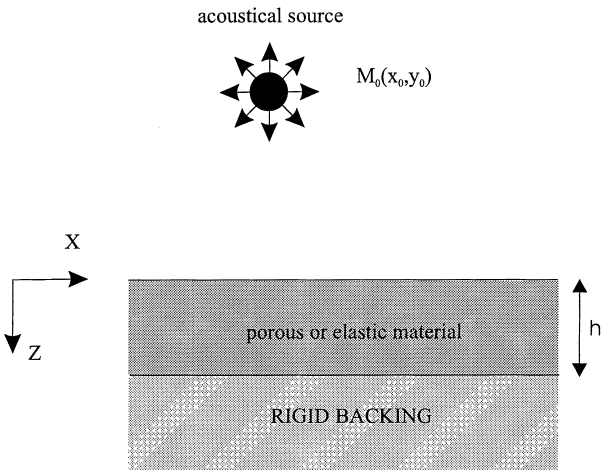

Fig. 1. Case of an acoustical line source radiating over a finite thick porous material.

$$\vec{\psi} = \frac{A_3(k_x)}{4\mathrm{i}\pi k_z^{\mathrm{S}}} \exp\left(-\mathrm{i}k_z^{\mathrm{S}} M - \epsilon \cdot z^{M_0}|\right), \tag{14}$$

where $=1$ for an ascending wave and -1 for a descending wave. A_i are the transmission coefficients in the porous medium for each kind of wave (these coefficients being different whether the wave is ascending or descending). $k_z^{\mathrm{P}i}$ and k_z^{S} are the vertical wave numbers in the porous medium depending on the kind of wave (the wave numbers are opposite for an ascending and a descending wave). The expressions of these wave numbers are given in Ref. [17].

For the case of an elastic material, $\hat{\Re}^i(k_x, z^M) = \{\hat{U}_S\}$ is expanded in propagation modes involving compressional and shear waves potentials, in the same way as previously. The expressions of these potentials are similar to the ones given in Eqs. (13) and (14), but the vertical wave numbers k_z^{P} and k_z^{S} are now those in the elastic medium.

In the case of a fluid, only compressional waves can propagate. The potential $\hat{\phi}$ associated with pressure P in the fluid has the same expression as in Eq. (13), considering the vertical wave number k_z^{P} in the fluid.

Once A_i have been determined, $\vec{\Re} \rightarrow_\omega (M)$ can be reconstructed using Eq. (9).

2.2.3. Calculation of the transmission and reflection coefficients

As said previously, the waves propagating in the different media are expanded in terms of propagation modes. The solid phase displacement and pressure inside the pores together with the acoustical pressure are expressed in terms of potentials whose expression involve reflection and transmission coefficients at each interface of the multi-layered material. These coefficients are determined by applying boundary conditions between materials. These conditions are given for various configurations by Deresiewieckz and Sfalak [19]. For an interface between two porous media, these are: (a) the solid phase normal displacement continuity, (b) the solid phase tangential displacement continuity, (c) the continuity of the normal relative displacement expressed as $\Phi(\vec{U}_S - \vec{U}_f)$, (d) the saturating fluid pressure continuity, (e) the solid phase normal strain continuity, (f) the solid phase tangential strain continuity. For a air-porous material interface, boundary conditions above are replaced by (a′) total normal displacement continuity, (d), (e), (f′) zero solid phase tangential constraint. For a porous-elastic material interface, these conditions are (a), (b), (c″) zero relative displacement in the porous material at the interface, (e″) normal total strain continuity, (f″) tangential total strain continuity. For boundary conditions in other configurations, the reader may refer to Ref. [19].

2.3. Numerical implementation

The calculation of $\exp(-\mathrm{i}\cdot k_x \cdot (x^M - x^{M_0}))\cdot \hat{\vec{\Re}}(k_x, z^M - z^{M_0})$ for the case of an infinitely thick porous material is now presented. The same process is used for a finite thickness or a multi-layered material.

Apart from the incident wave, another compressional wave is considered in air accounting for the reflected field. Two compressional and one shear waves, all descending, propagate in the porous medium. Fig. 2 summarizes the different waves involved. The calculation of $\exp(-\mathrm{i}\cdot k_x\cdot(x^M - x^{M_0}))\cdot\hat{\hat{\Re}}(k_x, z^M - z^{M_0})$ can be seen as the determination of the total response in air of the material (incident + reflected field) to an impinging plane wave excitation. For the sake of simplicity, a unit amplitude for the incident plane wave potential is assumed for this first step of the calculation. The potentials associated with each kind of wave have the following expression:

For the incident wave (*in air*)

$$\hat{\phi} = \exp(-\mathrm{i}\cdot k_x\cdot x)\cdot\exp\left(-\mathrm{i}\cdot k_z^{\mathrm{air}}\cdot z\right), \tag{15}$$

For the reflected wave (*in air*)

$$\hat{\phi}_{\mathrm{R}} = A_0\cdot\exp(-\mathrm{i}\cdot k_x\cdot x)\cdot\exp\left(+\mathrm{i}\cdot k_z^{\mathrm{air}}\cdot z\right), \tag{16}$$

where A_0 is the reflection coefficient on the interface.

For the transmitted waves (*in the porous material*)

P_1 wave

$$\hat{\phi}_{\mathrm{P}_1} = A_1\cdot\exp(-\mathrm{i}\cdot k_x\cdot x)\cdot\exp\left(-\mathrm{i}\cdot\gamma_{\mathrm{P}_1}\cdot z\right), \tag{17}$$

P_2 wave

$$\hat{\phi}_{\mathrm{P}_2} = A_2\cdot\exp(-\mathrm{i}\cdot k_x\cdot x)\cdot\exp\left(-\mathrm{i}\cdot\gamma_{\mathrm{P}_2}\cdot z\right), \tag{18}$$

S wave

$$\hat{\vec{\psi}} = A_3\cdot\exp(-\mathrm{i}\cdot k_x\cdot x)\cdot\exp(-\mathrm{i}\cdot\gamma_{\mathrm{S}}\cdot z), \tag{19}$$

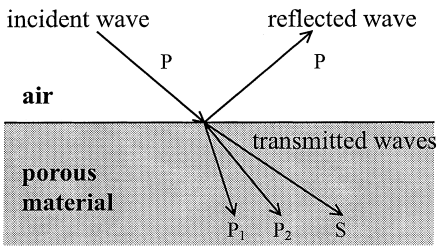

Fig. 2. Reflexion and transmission in a porous material for a plane wave excitation. The Biot Allard description of the porous material accounts for the propagation of txo compressional waves and a shear wave in the porous medium.

where, A_1, A_2, A_3 are the transmission coefficients associated with each kind of wave, and γ_{P_1}, γ_{P_2}, γ_S are the vertical wave numbers for P_1, P_2, S waves, respectively, in the porous material.

The boundary conditions between the porous material and air (conditions (a′), (d), (e), (f′)) are now expressed using the above potentials. These conditions yield:

$$\left[2\cdot\mu\cdot\gamma_{P_1}^2+\left(\lambda+(\alpha/\beta)\cdot(\alpha+\Phi\cdot(\mu_1-1))\cdot\delta_{P_1}^2\right)\right]\cdot A_1+\left[2\cdot\mu\cdot\gamma_{P_2}^2+\left(\lambda+(\alpha/\beta)\cdot(\alpha+\Phi\cdot(\mu_2-1))\cdot\delta_{P_2}^2\right)\right]\cdot A_2+2\cdot\mu\cdot k_x\cdot\gamma_S\cdot A_3=\rho_{air}\cdot\omega^2\cdot(1+R), \tag{20}$$

$$2\cdot\mu\cdot k_x\cdot\gamma_{P_1}\cdot A_1+2\cdot\mu\cdot k_x\cdot\gamma_{P_2}\cdot A_2+\mu\cdot\left(k_x^2-\gamma_S^2\right)\cdot A_3=0, \tag{21}$$

$$(1/\beta)\cdot[(\alpha-\Phi)+\Phi\cdot\mu_1]\cdot\delta_{P_1}^2+(1/\beta)\cdot[(\alpha-\Phi)+\Phi\cdot\mu_2]\cdot\delta_{P_2}^2=\rho_{air}\cdot\omega^2\cdot(1+R), \tag{22}$$

$$[(1-\Phi)+\Phi\cdot\mu_1]\cdot\gamma_{P_1}+[(1-\Phi)+\Phi\cdot\mu_2]\cdot\gamma_{P_2}+[(1-\Phi)+\Phi\cdot\mu_3]\cdot k_x=\gamma_{air}(1-R), \tag{23}$$

α, β are defined in Section 2.2.

The system formed by Eqs. (20)–(23) can by written in matrix form

$$[MC]\times[A_n]=[ML], \tag{24}$$

where $[A_n]$ is the vector of the reflection and transmission coefficients in the porous material. More generally, $[A_n]$ contains the reflection and transmission coefficients in the multi-layered material. $[MC]$ expresses the boundary conditions between reflected and transmitted waves. $[ML]$ is the incident wave vector. Each row of $[MC]$ and $[ML]$ corresponds to boundary conditions (20)–(23). Column i of $[MC]$ corresponds to a kind of wave considered in the multi-layered material and associated to the coefficient A_i. System (24) is solved using the Gauss pivot method. In that way, A_i are obtained and the scalar or vectorial response $\hat{\vec{\Re}}(k_x, z^M)$ is computed for any value of k_x and z, by multiplying coefficients A_i by the Green's function amplitude coefficient (see Eq. (11)).

2.3.1. *Computation of* $\vec{\Re}_\omega^i(x,z)$ *from* $\hat{\vec{\Re}}(k_x, z^M)$

To compute the fields in the different media, an inverse wave number transform must be performed on $\hat{\vec{\Re}}^i(k_x, z)$(see Eq. (9)). However, this inverse wave number transform cannot be performed analytically and a numerical method has to be applied. The discrete wave number method, referred to as Bouchon's method [20],

and used in seismology, is proposed. In this method, the field radiated by a unique source is approached by the field created by an infinite set of periodic sources S_ω. These latter sources are periodic along one axis, parallel to the interface, and distant from each other of distance L (see Fig. 3). By construction, each source of this set is a superposition of plane waves. The angular spacing between the propagation direction of two consecutive plane waves is linked to L by Eq. (28). L tending to infinity corresponds to a unique source. The response to a periodic set of sources is also periodic with the same period L. The approximation of the field $\vec{\Re}^i_\omega(M)$ radiated by a unique source is obtained by adding the contributions of all the periodic sources $\vec{\Re}^i_\omega(O_j, M)$, where O_j is the position of the periodic source j. Its expression is given by

$$\vec{\Re}^i_\omega|_{\text{periodized}}(M) = \sum_{j=-\infty}^{+\infty} \vec{\Re}^i_\omega(O_j, M). \tag{25}$$

By using Eq. (9) for each term of the sum in Eq. (25), the response at $M(x_1,x_3)$ can finally be expressed as [20]

$$\vec{\Re}^i_\omega(M) \approx \vec{\Re}^i_\omega|_{\text{periodized}}(M) = \sum_{n=-\infty}^{n=+\infty} \exp(-\mathrm{i}\cdot k_n \cdot x)\cdot \hat{\vec{\Re}}(k_n, z)\cdot \Delta k, \tag{26}$$

with

$$k_n = n\cdot \Delta k \tag{27}$$

and

$$\Delta k = \frac{2\pi}{L}. \tag{28}$$

The horizontal wave number k_x has only discrete values (Eq. (27)), and the spectral spacing Δk is linked to L (Eq. (28)). Practically, Eq. (26) becomes a finite sum, with a summation index varying from $-N_{\max}$ to $N_{\max}$. Both values of $N_{\max}$ and L will be important for the convergence of the approximation of Eq. (26). First, the periodic length L must be large enough to insure that the discretization of the wave number

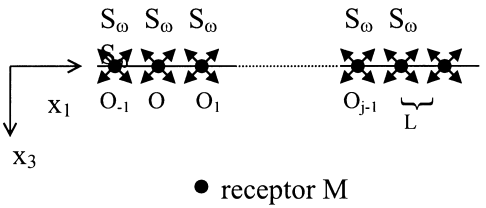

Fig. 3. Bouchon's method theoretical principal. The initial source is replaced by a set of infinite sources radiating in discrete directions.

spectrum leads to a suitable approximation of $\hat{\hat{\Re}}_{\omega}(k_x, x_3)$. Also N_{max} must be large enough so as to take into account at least all significant contributions, i.e. homogenous and evanescent wave contribution. Suitable values for $N_{\max}$ will be discussed later.

The expression obtained for the approximation of the fields using a set of periodic sources is equivalent to the computation of the response in the material by performing the calculation in one point of a set of receivers by an inverse discrete Fourier transform (IDFT) instead of a calculation of this response by direct integration for that receiver as expressed in Eq. (9). In that way, the use of an IFFT algorithm can be considered in order to "optimize" Bouchon's method, and the fields are computed on a grid of receivers parallel to the air–porous interface. For each receiver M_j with coordinates z fixed and $x_j = j\cdot\Delta x$ ($j=-N_{\max},N_{\max}$), expression (26) is then approximated by

$$\vec{\Re}_{\omega}(M_j) \approx \sum_{n=-N_{\max}}^{n=+N_{\max}} \exp(-\mathrm{i}\cdot k_n \cdot x^{M_j})\cdot\hat{\hat{\Re}}(k_n, z)\cdot\Delta k. \tag{29}$$

This expression can either be processed with for each receiver M_j or with an IFFT algorithm using the array $\left\{\hat{\hat{\Re}}(k_j, z)\cdot\Delta k\right\}_j$ ($j=-N_{\max},N_{\max}$). However if an IFFT algorithm is used, the positions of the receivers and their spatial spacing will be determined once Δk and $N_{\max}$ are given. We have $x_{1j}=j\times\Delta x(j=-N_{\max},N_{\max})$ with $\Delta x=2\pi/k_{\max}$, and $x_{\max}=\pi/(\Delta k)$ according to the Shannon criterion. Δk and $N_{\max}$ are chosen so as to insure the convergence of the approximation (29).

The algorithm presented above allows for the computation of any fields at any point of a multi-layered material. The characteristics of the material such as surface impedance or the transmission loss for either a plane wave or a line source excitation can also be calculated.

3. Validation and numerical results

Basically, the developed algorithm requires solving a series of plane wave problems associated with the discrete wave number k_j. Firstly, the validation of the calculation of $\hat{\hat{\Re}}_{\omega}(k_x, x_3)$ is considered. Then, some validation results regarding the computation of pressure levels due to an acoustical line source radiating over a porous material are presented together with some original results.

3.1. Calculation of $\hat{\hat{\Re}}^{i}(k_x, z)$

The first example considers a plate-mineral wool-plate system, infinite in two of its dimensions and surrounded by air on each side (see Fig. 4). The characteristics of the materials are given in Table 1. The excitation is an impinging plane wave under

normal incidence. Fig. 5 compares the transmission loss for this configuration obtained with the developed algorithm and those obtained by an analytical formula of Lesueur [21]. The latter approach originally considered a fluid between the two plates. In the present example, the characteristics of the fluid are those of the porous material depicted by the equivalent fluid Biot–Allard [3] model using characteristic

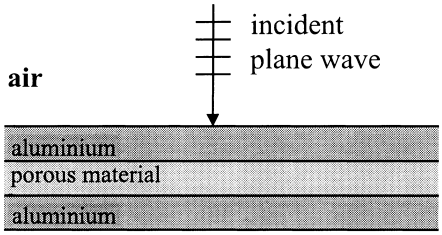

Fig. 4. Configuration of a sandwich plate excited by an impinging plane wave.

Table 1
Characteristics of aluminium (first line) and the porous material (second line)

Young modulus (Pa)	7.1×10^{10}
Poisson's coefficient ν	0.3
Volumic mass (kg/m^3)	2814
Thickness (cm)	1×10^{2}
α_∞ (Tortuosity)	1.2
Φ(Porosity)	0.925
ρ_1 (kg/m^3)	43
$\sigma(N \times \text{s/m}^4)$	70,000
Λ (m)	3×10^{5}
Λ' (m)	8×10^{5}
Thickness (m)	2×10^{2}

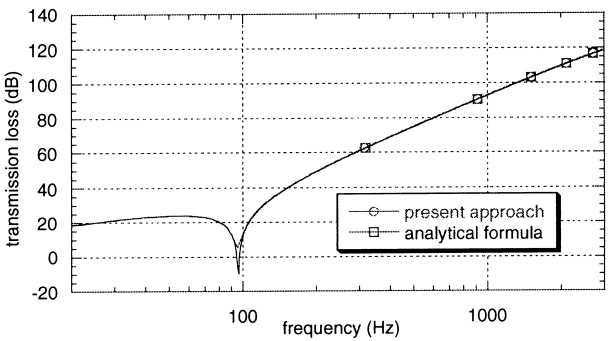

Fig. 5. Prediction of the transmission loss for the sandwich plate using Lesueur's analytical formula and the present approach. The porous medium is modeled as an equivalent fluid in both cases.

Table 2
Characteristics of the different layers used in Fig. 5

	α_∞	ρ_1 (kg/m^3)	σ ($N \times$ s/m^4)	Φ	N (N/cm^2)	ν	Λ (m)	Λ' (m)	Thickness (cm)
Material 1	1.18	41	34×10^3	0.98	$11 \times (1 + j \times 0.015)$	0.3	60×10^{-6}	87×10^{-6}	0.4
Material 2	2.56	125	3.2×10^6	0.80	$100 \times (1 + j \times 0.1)$	0.3	6×10^{-6}	24×10^{-6}	0.08
Material 3	2.52	31	87×10^3	0.97	$5.5 \times (1 + j \times 0.055)$	0.3	37×10^{-6}	119×10^{-6}	0.5
Material 4	1.98	16	65×10^3	0.99	$1.8 \times (1 + j \times 0.1)$	0.3	37×10^{-6}	121×10^{-6}	1.6

viscous and thermal length. The same model has been used in the proposed algorithm for the porous material. The results on Fig. 5 show a very good agreement between the proposed model and the analytical solution.

The second example considers a porous material made up of four different layers (see characteristics in Table 2) of finite thickness bonded onto a rigid wall. The poroelastic structure is excited by an impinging plane wave under normal incidence. The real and imaginary part of the surface impedance of the structure are computed using the developed approach. The results are compared to those given by Panneton and Atalla [7] for a finite element model, on Fig. 6. An excellent agreement is obtained between the two models. Moreover, both of them emphasize the importance of taking into account the frame movement. Actually they highlight resonance phenomenon around 500 Hz that would not have been apparent with an equivalent fluid model.

In the following, a line source in air radiating over a porous material is considered. The noise levels at any point will be predicted using the fields approximation presented in Section 2.3.

3.2. Study of the different parameters influential on the convergence

As was seen in Section 2.3, Eq. (29) provides an approximation of the fields whose computation can be optimized by the use of an IFFT algorithm. However, criteria are to be found for the convergence of this approximation.

3.2.1. Criterion on k_{max}

The configuration represented on Fig. 7 is considered with the infinite thickness foam depicted in Table 1. The levels are calculated for a receiver at the interface, right under the source at distance $d = 0.5$ m, using Bouchon's method with $L = 500$ m for the considered frequency range. First of all, a suitable value for $k_{\max}$ has to be found to insure the convergence of the sum approaching the field. Fig. 8 represents

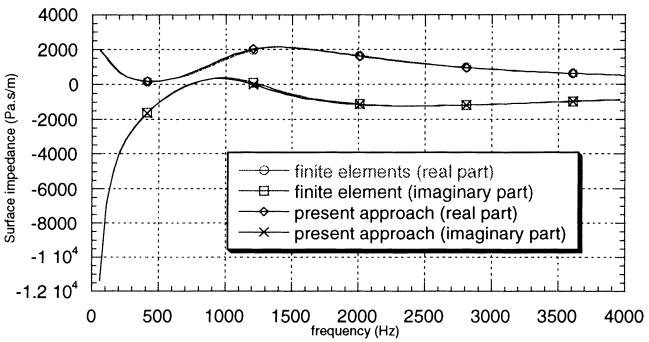

Fig. 6. Case of a finite thick multilayered material excited by a plane wave with normal incidence. The surface impedance is predicted by FEM and the present approach with Biot Allard description of the porous media.

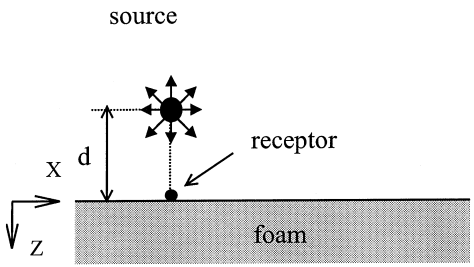

Fig. 7. The different parameters influential on the convergence of Bouchon's method approximation. Source receiver configuration.

the results as a function of frequency with a value for $k_{\max}$ varying between $0.95 \times \omega/C_{\text{air}}$ and $1.5 \times \omega/C_{\text{air}}$. As one could have expected, it appears that all contributions for $k_x < \omega/C_{\text{air}}$ must be taken into account. Actually, these values for k_x correspond to propagating plane waves, so that they cannot be neglected. The value $k_{\max} = 1.3 \times \omega/C_{\text{air}}$ seems to insure convergence of the computed field. Studies made on other materials give similar values for $k_{\max}$ for the considered source-receiver configuration.

The second parameter that influences convergence of the sum is the position of the receiver $M(x,z)$ with respect to the source $M_0(0,z_0)$. It appears that when the source-receiver distance is large, i.e. $-z_0| \gg 1$, the required value for $k_{\max}$ gets close to ω/C_{air}. Also the x coordinate of the receiver (the source is assumed to be at the x-axis

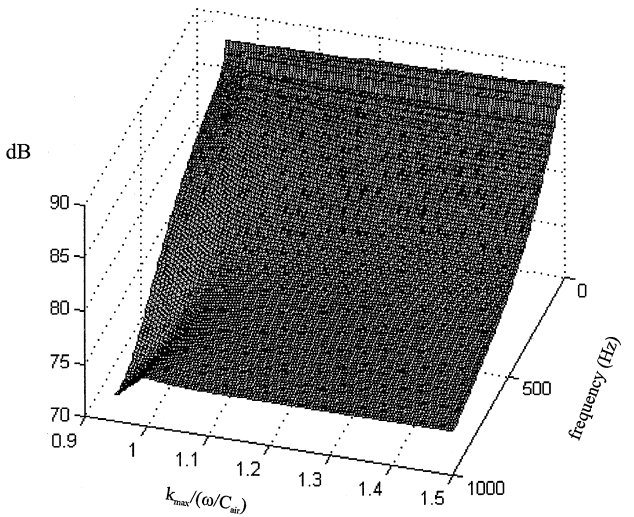

Fig. 8. Suitable frequency dependant values for $k_{\max}$ to insure the convergence of Bouchon's method approximation of the fields. A fixed $k_{\max}/(\omega/C_{\text{air}})$ ratio can be determined for the frequency range considered.

origin) has little influence on the required k_{max}. Actually, considering the previous remarks, the criterion $k_{max} = 2 \times \omega / C_{air}$ is so applied for all configurations and materials to insure convergence.

3.2.2. *Criterion on* N_{max}

The second criterion of convergence lies in the number N_{max} of terms, or equivalently the wave number spacing Δk ($= k_{max}/N_{max}$) chosen for either a term by term calculation or the IFFT algorithm. When considering the physical approach of Bouchon's method, Δk is linked to the periodization length L. Obviously, the number of sampling values for the approximation is the important parameter. Consequently, values of L for convergence are frequency dependent.

Moreover, required values for N_{max} also depend on the distance between the source and the receiver and the kind of material. This latter dependency is highlighted by a study on two materials described in this section. A foam with characteristics given in Table 1, and a soil with a characteristics given in Table 3, are considered, both having with infinite thickness. Suitable values of N_{max} vary from 300 to 1100 for the foam and from 300 to 1700 for the soil when the distance between the source and receiver varies from 0 to 500 m.

3.3. *Validation of* $\vec{\Re}^i_\omega(M)$

An acoustic line source radiating over an infinite foam is examined. The characteristics of the foam are given in Table 1. Fig. 9 displays the sound levels are

Table 3
Characteristics of the soil

α_∞	Φ	ρ_S (kg/m^3)	σ ($N \times$ s/m^4)	Shape factor	Thickness (m)
1.93	0.269	2650	366 000	1.38	∞

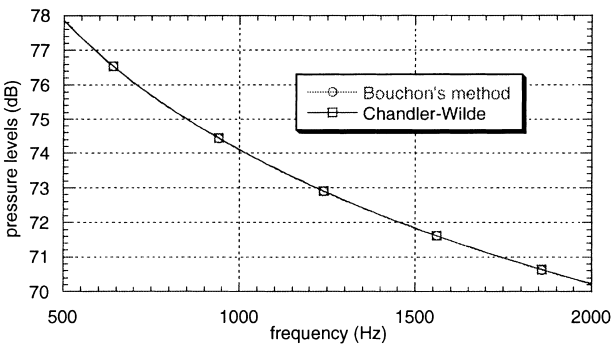

Fig. 9. The use of Bouchon's method for the prediction of pressure levels due to a line source radiating over a semi infinite thick foam, modeled as an equivalent fluid. The receiver is straight below the source, at the air porous interface. The results are compared to those given by Chandler Wilde's analytical formula.

computed for a receiver on the interface, right under the source at distance $d = 0.5$ m using Bouchon's method and Chandler–Wilde's analytical formula [15]. For the first method, $k_{max} = 2\omega/(C_{air})$ and a value of $L = 500$ m have been chosen. Since Chandler–Wilde's approach requires to consider the material as locally reacting, Delany–Bazley model was utilized to characterize the foam for the analytical comparison. In the developed approach, the Biot–Allard model mentioned earlier was chosen. The two models used give close descriptions of the porous materials in this case except perhaps at low frequencies. The results are represented on Fig. 9. Agreement between the two approaches is excellent.

3.4. Efficiency of the optimization of Bouchon's method by IFFT algorithm

In the present case, pressure levels due to a line acoustic source are calculated on a grid of receptors at the air–porous interface. The same material as in the previous example is considered. The results computed at 1000 Hz are represented on Fig. 10, as a function of the distance from the source. There is a good agreement between IFFT and the point by point calculation for the considered distances. However, the results given by IFFT are erroneous when getting close to x_{max}. This phenomenon is known as aliasing. This is due to the fact that IFFT algorithm requires that the field vanishes outside out of the range interval considered, which is not the case here. From there, the field out of this range interval will be wrapped around in the neighboring windows. This means that the field calculated in the receptors will be the sum of the signals in all range windows having the same width as the studied range interval. As far as the horizontal wave number spectrum is concerned, this phenomenon can be accounted for by an undersampling of the spectrum in the neighborhood of a pole of the integrand in Eq. (9). Improvements can be reached by adaptative integration scheme, or complex integration paths of Eq. (9). These techniques are described elsewhere [22].

To conclude, an IFFT algorithm can be used rather than a point by point computation to solve in a more efficient way the considered problem with a plane interface,

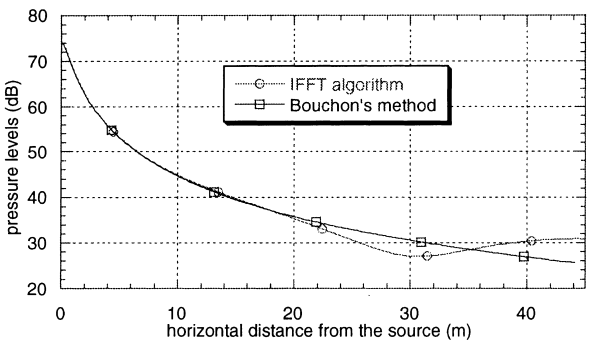

Fig. 10. Computation of pressure levels on a grid of receivers at 1000 Hz. Results are represented for a point by point and an optimization by the use of an IFFT algorithm.

Table 4
Characteristics of the foam

α_∞	Φ	ρ_1 (kg/m^3)	N(N·m^{-2})	ν (Poisson's coefficient)	σ (N × s/m^4)	Λ' (m)	Λ' (m)	Thickness (m)
1.2	0.925	43	N	$102000 + j \times 6000\ \nu$	0.45	70 000	3×10^{-5}	8×10^{-5}	5×10^{-2}

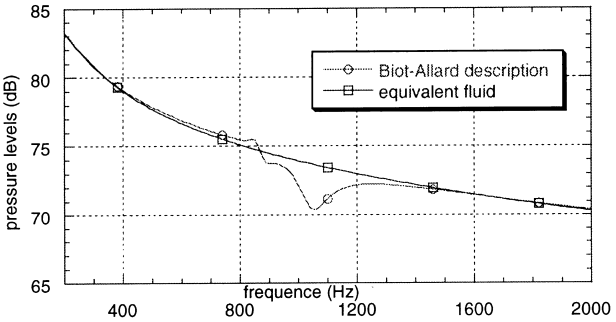

Fig. 11. Case of a finite thick foam on a rigid backing. Influence of the solid phase motion on the pre diction of pressure levels for a line source excitation. Quarter wave resonances for a complete description of the porous medium is highlighted.

as far as the computational time is concerned. However, Bouchon's method is of great interest since it give a physical background to what could be seen as a simple integration scheme.

3.5. Numerical results for an acoustical line source

Finally a configuration of a finite thickness foam on a rigid support and excited by a line source is considered. The same emitter–receiver configuration as for the previous example is chosen. The characteristics of the foam are given in Table 4. The levels at the receiver are given by Bouchon's method. A periodization length $L = 500$ m has been taken to insure convergence in the considered frequency range. The results are represented on Fig. 11. In this case, the influence of the frame motion is studied. These results show resonance peaks at about 900 Hz which highlight the importance of taking into account the frame motion. Outside of these resonances, the levels are very similar for the frequency range studied, with or without accounting for skeleton motion.

4. Conclusion

This paper investigated the prediction of the fields induced by an acoustical line source exciting an infinite lateral multi-layered material with an infinite planar

interface. The first original aspect of this work is to take into account the propagation phenomena in the whole material. In particular, a complete description of porous materials based on Biot–Allard equations was employed. The second aspect is related to the method used to solve the problem, namely Bouchon's method. In this method, the fields created by the original source are approached by those induced by a set of infinite sources radiating in discrete directions. These sources are periodic along the axis parallel to the interface, and the interspacing is related to the angular spacing of the discrete directions in which they emit. An IFFT algorithm can also be used to compute the levels on a grid of receptors from the values of the Fourier transform of the fields in a finite numbers of points.

The Fourier transform of the transmitted and reflected fields computed by the implemented algorithm has been validated. Several types of materials were considered: sandwich plates with porous material in-between, finite thickness porous multi-layered material bonded on a rigid wall. The results obtained are in complete agreement with analytical formulas or other numerical method found in the literature and testify to the reliability of the algorithm. Moreover, the second case studied also highlighted the limits of the motionless frame hypothesis, which had already been underlined in literature.

For a line source excitation, Bouchon's method was used. The results obtained are again in excellent agreement with those given by an analytical solution for the case of a porous material considered as locally reacting. Besides, the importance of the frame movement was demonstrated once again in the case of a finite foam on a rigid backing. Criteria have been established to insure the convergence of the fields approximations. First, the reconstruction of the fields requires accounting for all significant contributions in the sums approaching the fields expression. In that way, the criterion $k_{\max} > (2 \times \omega / C_{\max})$ was met. Also, a large periodization length L, linked to Δk, had to be taken. For a given frequency, suitable values for $N_{\max}$ highly depend on the source-receiver distance and the material. The use of an IFFT allowed for an optimization of the designed algorithm in terms of computational time. But then, the fields are processed on grid of receivers and a minimal width $x_{\max}$ is imposed when a maximum Δk at fixed $k_{\max}$ is chosen, since $x_{\max} = \pi/(\Delta k)$.

The quality of the results obtained enables one to think about Bouchon's method for an irregularly shaped air–material interface. In particular, future works could consist in finding the response of a linear source radiating over a road coupled with a soil of any profile. This particular problem finds applications in outdoor sound propagation, where one intends to predict sound levels near a roadway. Bouchon's method has already been used for similar configurations in seismology [23]. The approach consists in replacing the profile by a set of periodic sources with unknown amplitudes distributed on the interface, both in air and in the material. The whole configuration obtained is then periodized in one direction, the same way as was done in this paper. In that way, a periodic profile which has to be known on the whole periodization length L is considered. This "double periodization" leads to an approximation of the fields by a double sum. Bouchon's method could also be employed for a mechanical line force acting on a multi-layered porous material [17]. In this case, the source is considered to lie just slightly below the interface. So rather

than an acoustical source one has to deal with a poro-elastic or elastic source according to the kind of material excited. The fields in the excited medium are then determined as was done in this paper. The only changes concern the incident fields; the amplitudes of each propagation mode are related to Green's coefficients in the excited medium.

References

[1] Zwikker C, Kosten CW. Sound absorbing materials. New York: Elsevier, 1949.
[2] Sabatier JM, et al. The interaction of airborne sound with the porous ground: The theoretical for mulation. J Acoust Soc Amer 1986;79(5):1345 52.
[3] Allard, J F. Propagation of sound in porous media. Modelling sound absorbing materials, vol. 1. London: Elsevier, 1993:284.
[4] Tooms S, Attenborough K. Propagation form a point source above a porous and elastic foam layer. Applied Acoustics 1993;39:53 63.
[5] Stoll RD. Theoretical aspects of sound transmission in sediments. J Acoust Soc Amer 1980;68:1341 50.
[6] Bolton YJ, Kang, JS. Finite element modeling of isotropic elastic porous materials coupled with acoustical finite elements. J Acoust Soc Amer 1995;98(1):635 43.
[7] Panneton R, Atalla N. An efficient finite element scheme for solving the three dimensional por oelasticity problem in acoustics. J Acoust Soc Amer 1997;101:1 12.
[8] Atalla N, Debergues P. Validation of examples for the mixed pressure displacement formulation for poroelastic media. University of Sherbrooke: Sherbrooke, 1997.
[9] Nobile, MA, Hayek SI. Acoustic propagation over an impedance plane. J Acoust Soc Amer 1985;78(4):1325 36.
[10] Habault D, Filippi PJT. Ground effect analysis: surface wave and layer potential representations. J Sound Vibration 1981;79(4):529 50.
[11] Habault D, Filippi PJT. Sound propagation over ground: analytical approximations and experi mental results. J Sound Vibration 1981;79(4):551 60.
[12] Attenborough K, Richards TL. Solid particle motion induced by a point source above a poroelastic half space. J Acoust Soc Amer 1989;86(3):1085 91.
[13] Tooms S, Taherzadeh S, Attenborough K. Sound propagation in a refracting fluid above a layered fluid saturated porous elastic material. J Acoust Soc Amer 1993;93(1):173 81.
[14] DiNapoli FR, Davenport RL. Theoretical and numerical Green's function solution in a plane layered medium. J Acoust Soc Amer 1980;67:92 105.
[15] Chandler Wilde SN. Ground effects in environmental sound propagation, in Civil and structural engineering. University of Bradford: Bradford, 1988:702.
[16] Boutin C, Bonnet G, Bard PY. Green functions and associated sources in infinite and stratified poroelastic media. Geophys J R Astr Soc 1987;90:521 50.
[17] Boutin C. Dynamique des milieux poreux saturés déformables. fonctions de Green Perméamètre dynamique, in Institut mecanique de Grenoble. Université scientifique, technologique et médicale de Grenoble: Grenoble (France), 1987.
[18] Brouard B, et al. Measurements and prediction of the reflection coefficient of porous layers at obli que incidence and for inhomogeneous waves. J Acoust Soc Amer 1996;99(1):100 7.
[19] Deresiewieckz H, Sfalak R. On uniqueness in dynamic poroelasticity. Bull Seism Soc Amer 1963;53:783 8.
[20] Bouchon M. Calculation of complete seismograms for an explosive source in a layered medium. Geophysics 1980;45(2):197 203.
[21] Lesueur C. Rayonnement acoustique des structures. Collection de la direction des etudes et recher ches d'Electricité de France. Paris: Editions Eyrolles, 1988:591.

[22] Jensen FB, et al. Computational ocean acoustics. AIP Series in Modern Acoustics and Signal Processing, New York: American Institute of Physics, 1994:612.
[23] Campillo M, Bouchon M. Synthetic SH seismograms in a laterally varying medium by the discrete wavenumber method. Geophys J R Astron Soc 1985;83(1):307.